Commun. Comput. Phys.
doi: 10.4208/cicp.2009.09.065

Vol. **8**, No. 1, pp. 143-158
July 2010

Unstable Surface Modes in Finite Chain Computations: Deficiency of Reflection Coefficient Approach

Shaoqiang Tang* and Ming Fang

Center for Applied Physics and Technology, and LTCS, College of Engineering, Peking University, Beijing 100871, China.

Received 9 April 2009; Accepted (in revised version) 5 October 2009

Available online 12 February 2010

Abstract. In this paper, we investigate the stability for a finite harmonic lattice under a certain class of boundary conditions. A rigorous eigenvalue study clarifies that the invalidity of Fourier modes as the basis results in the deficiency of standard reflection coefficient approach for stability analysis. In a certain parameter range, unstable surface modes exist in the form of exponential decay in space, and exponential growth in time. An approximate eigen-polynomial is proposed to ease the stability analysis. Moreover, the eigenvalues with small positive real part quantitatively explain the long time instability in wave propagation computations. Numerical results verify the analysis.

PACS: 43.20.+g, 83.10.Rs, 63.20.D-

Key words: Unstable surface mode, reflection coefficient, finite chain.

1 Introduction

Interfaces/surfaces are of fundamental importance in materials science and engineering. Substantial understanding of the physics has been obtained through studies on wave propagations across an interface/surface. Generally speaking, the two materials across an interface/surface yield different dispersion relations. Continuity of the wave function requires a certain combination of waves with different propagation directions. Wave features are then usually characterized by the reflection and transmission coefficients. In the mean time, interfaces/surfaces also play an important role in numerical computations. For instance, in a multi-scale computation that couples atomistic dynamics and continuum deformation, atomistic fluctuations need to be damped out through suitable boundary conditions. As it is virtually impossible to cleanly transmit all fluctuations, the reflected part enters back and cause spurious wave interactions inside the atomistic

*Corresponding author. *Email address:* maotang@pku.edu.cn (S. Tang)

domain. Hence a key ingredient for a multi-scale algorithm is the design of interfacial conditions for reflection reduction. In the literature, numerical absorption treatments have been proposed, including a perfect matched layer, or a time history kernel convolution, or a velocity interfacial condition, etc [1,5,20,23–25]. Most of these methods adopt a sinusoidal Fourier mode viewpoint, and are validated or analyzed through the resulted reflection coefficients. A dynamic atomistic-continuum algorithm is even designed by minimizing the reflection coefficient within a certain range of wave-numbers [6]. In addition, for continuous wave propagation in an unbounded domain, one assigns a finite computing domain. Numerical boundary conditions are then also analyzed and optimized through the reflection coefficient approach [3,7,10,12,13,17,27]. We remark that rigorous analysis had also been performed for continuous wave equations by Kreiss and others [8,14], and for discrete schemes by Halpern, Li, and others [9,15].

In this paper, we study carefully the validity of the reflection coefficient approach for wave propagation applications. As is known for a long time, the Fourier modes do not completely or accurately describe the wave features for finite lattice chains. We quantitatively demonstrate, with a velocity interfacial condition, that this invalidity results in the deficiency of the reflection coefficient approach and incorrect stability results. We observe unstable surface modes in a parameter range where the reflection coefficient approach claims to be stable. An approximate eigen-polynomial is proposed, which has a much lower order than the full problem. This may greatly ease a rigorous stability analysis. The eigen modes are classified into unstable surface modes, absorption modes, and vibration/propagation modes. Our results reveal the complexity of wave propagations in multiple media, and urges for substantiating numerical analysis for multi-scale computations. We remark that the finite size effects may lead to possible discoveries for micro-/nano-materials, similar to those for electronic states in a finite crystal [22].

The rest of the paper is arranged as follows. We describe the governing equations and the reflection coefficient approach for a finite chain in Section 2. Then a full eigen-problem study is performed in Section 3. Numerical tests are also presented. In Section 4, we discuss long time instability, which is a subtle issue in numerical simulations and quantitatively explained by the current eigen-problem results. We make some concluding remarks in Section 5.

2 Reflection coefficient

We consider a harmonic lattice consisting $(N+2)$ atoms. The n-th atom deviates from its equilibrium by a displacement $u_n(t)$, and a velocity $v_n(t)=\dot{u}_n(t)$. We impose the same type of boundary conditions at both ends. The governing system is as follows.

$$\dot{u}_0=\alpha u_0+\beta u_1, \tag{2.1a}$$

$$\dot{u}_n=v_n, \quad n=1,\cdots,N, \tag{2.1b}$$

$$\dot{v}_n=u_{n-1}-2u_n+u_{n+1}, \quad n=1,\cdots,N, \tag{2.1c}$$

$$\dot{u}_{N+1} = \alpha u_{N+1} + \beta u_N. \tag{2.1d}$$

Here α and β are constants. In a reflection coefficient approach, one actually considers a semi-infinite chain instead, e.g., $n = 0,1,2,\cdots$. A monochromatic wave is decomposed into a transmission component and a reflection component.

$$u_n(t) = e^{i(\omega t - kn)} + Re^{i(\omega t + kn)}. \tag{2.2}$$

From the Newton equations of the inner atoms, the frequency ω and the wave number $0 \le k \le \pi$ are related by the dispersion relation $\omega = 2\sin(k/2)$. Substituting this into the boundary condition, we obtain the reflection coefficient

$$R(k) = -\frac{(\alpha + \beta\cos k) + i(\beta\sin k - 2\sin(k/2))}{(\alpha + \beta\cos k) + i(\beta\sin k + 2\sin(k/2))}. \tag{2.3}$$

From this expression, it is obvious that $|R| < 1$ for $\beta > 0$, and $|R| > 1$ for $\beta < 0$. For a finite chain, it is widely conceived that $|R| < 1$ indicates energy decay and hence stability. A possible interpretation is as follows. When a localized one-way wave package reaches at the boundary, each Fourier mode is partially transmitted. Because $|R| < 1$, the reflection part has a smaller amplitude than the incident wave, and alternates the propagation direction. By virtue of the Parseval's relation, the whole reflection wave package has a smaller energy. The energy repeatedly decreases when the wave package reaches at either end. By a similar argument, instability is expected if $|R(k)| > 1$ for a certain range of k.

This interpretation assumes the Fourier mode decomposition. Later we shall compute the eigen-modes, which turn out to be not the Fourier modes for the finite chain with generic boundary conditions. In particular, because instability emerges in the form of non-Fourier modes, the reflection coefficient approach may not be suitable for the stability analysis.

In solid state physics, an infinite periodic lattice is usually assumed. Though it is known for long time that a real finite lattice does not possess the Fourier eigen modes, the deviation is not precisely identified, and is believed to be negligible for a lattice big enough. On the other hand, for a multiscale computation, the finite lattice considered here corresponds to the atomistic subdomain, where fine scale calculations are performed. A surrounding infinite periodic lattice is assumed to be at equilibrium initially. If an exact/transparent interfacial condition is posed, e.g., in the time history convolution form, the Fourier modes still serve as the basis provided that the atomistic subdomain has the same lattice structure. However, this does not hold when either a non-exact interfacial condition is adopted due to time cut-off or discretization error, or the atomistic subdomain has a different lattice structure. For such cases, the eigen modes are not in the form of Fourier modes in the atomistic subdomain, even if they are so in the surrounding lattice. Moreover, the atomistic subdomain together with the interfacial condition forms a closed system. With the bridging scale technique, for instance, this closed system describes the fluctuation part of the motion in the atomistic subdomain. For both theoretical

and numerical error analysis of interfacial conditions, one actually considers the reflection of the atomistic subdomain. Therefore, a substantial understanding of the dynamic system (2.1a)-(2.1d) is crucial for both the physics and the multiscale computations.

3 Eigenvalue study for finite chain

We perform a complete eigenvalue study to substantiate the understanding on wave properties of the finite chain.

3.1 Eigenvalue problem

Since the governing system is linear, we may find the eigenvalues and eigenvectors for the coefficient matrix on the right hand side. The motion of the lattice is then explicitly expressed as a superposition of these eigen-modes.

In addition to the standard matrix approach, an eigen-mode may also be obtained as a solution in the form of $u_n(t)=\tilde{u}_n e^{\lambda t}$ and $v_n(t)=\lambda\tilde{u}_n e^{\lambda t}$. The time-independent variables $\{\tilde{u}_n\}$ solve

$$\lambda\tilde{u}_0=\alpha\tilde{u}_0+\beta\tilde{u}_1, \tag{3.1a}$$

$$\lambda^2\tilde{u}_n=\tilde{u}_{n-1}-2\tilde{u}_n+\tilde{u}_{n+1},\quad n=1,\cdots,N, \tag{3.1b}$$

$$\lambda\tilde{u}_{N+1}=\alpha\tilde{u}_{N+1}+\beta\tilde{u}_N. \tag{3.1c}$$

From (3.1b), we have a general expression for $\{\tilde{u}_n\}$ as follows:

$$\tilde{u}_n=Aq_+^n+Bq_-^n. \tag{3.2}$$

Here

$$q_\pm=[\lambda^2+2\pm\lambda\sqrt{\lambda^2+4}]/2\neq 0$$

are the two roots to

$$q^2-(\lambda^2+2)q+1=0. \tag{3.3}$$

Substituting this into (3.1a) and (3.1c), we find that the coefficients A and B satisfy

$$\begin{bmatrix} \lambda-\alpha-\beta q_+ & \lambda-\alpha-\beta q_- \\ (\lambda-\alpha)q_+^{N+1}-\beta q_+^N & (\lambda-\alpha)q_-^{N+1}-\beta q_-^N \end{bmatrix}\begin{bmatrix} A \\ B \end{bmatrix}=0. \tag{3.4}$$

Nontrivial solutions A and B exist only when the coefficient matrix is singular. Due to $q_-q_+=1$, the condition amounts to

$$-q_-^{N+1}\Big\{[(\lambda-\alpha)q_+-\beta]q_+^N+[\lambda-\alpha-\beta q_+]\Big\}\Big\{[(\lambda-\alpha)q_+-\beta]q_+^N-[\lambda-\alpha-\beta q_+]\Big\}=0. \tag{3.5}$$

The eigenvalues are therefore roots to the eigen-polynomials

$$V_N^\pm(\lambda)=q_+^N[(\lambda-\alpha)q_+-\beta]\pm[\lambda-\alpha-\beta q_+]=0. \tag{3.6}$$

In particular, for an eigenvalue λ that is a root to $V_N^+(\lambda)$, it holds that $\lambda-\alpha=\beta(q_+^N+q_+)/(q_+^{N+1}+1)$. We take

$$A=(\lambda-\alpha-\beta q_-)\frac{q_+^{N+1}+1}{\beta(q_+^{N+1}-q_+^{N-1})},\quad B=[-(\lambda-\alpha)+\beta q_+]\frac{q_+^{N+1}+1}{\beta(q_+^{N+1}-q_+^{N-1})}. \tag{3.7}$$

After some algebra, we compute the eigenvector as

$$\tilde{u}_n=q_+^{-n+1}+q_+^{n-N},\quad n=0,\cdots,N+1. \tag{3.8}$$

Because $\tilde{u}_{N+1-n}=\tilde{u}_n$, the eigenvector is symmetric.

Next, we check the eigenvalues and eigenvectors in more details. Let $q=\rho e^{i\theta}$. We may rewrite equation (3.3) as

$$\lambda=\pm(q^{1/2}-q^{-1/2})=\pm\left[(\sqrt{\rho}-\frac{1}{\sqrt{\rho}})\cos\frac{\theta}{2}+i(\sqrt{\rho}+\frac{1}{\sqrt{\rho}})\sin\frac{\theta}{2}\right]. \tag{3.9}$$

Therefore, for an eigenvalue λ with $|\mathrm{Re}\lambda|$ not small, the corresponding $|q_+|$ is away from 1 by an amount not small. There are two consequences for such an eigenvalue. First, the components of the corresponding eigenvector are negligible for n not close to 0 or $(N+1)$, compared with the components

$$\tilde{u}_0=\tilde{u}_{N+1}=q_++q_+^{-N}.$$

In addition, the components for n close to 0 or $(N+1)$ decay on the order of q_+^{-n+1} or q_+^{n-N}. The eigen-mode is therefore a kind of surface mode, decaying exponentially in space away from the surface. Secondly, because either $|q_+^N|\gg 1$ or $|q_+^N|\ll 1$ in (3.6) for a chain long enough, the eigenvalue approximately solves either

$$(\lambda-\alpha)q_+-\beta=0, \tag{3.10}$$

or

$$(\lambda-\alpha)-\beta q_+=0. \tag{3.11}$$

In both cases, λ is approximately a root to the cubic polynomial

$$\beta\lambda^3-(1+\alpha\beta)\lambda^2+2(\alpha+\beta)\lambda-(\alpha+\beta)^2=0, \tag{3.12}$$

subject to the constraint

$$|\lambda-\alpha|<|\beta|. \tag{3.13}$$

This serves as a simplified eigen-polynomial for stability analysis. Compared with (3.6), it has a much lower order.

Similarly, for an eigenvalue λ that is a root to $V_N^-(\lambda)$, it holds that $\lambda-\alpha=\beta(q_+^N-q_+)/(q_+^{N+1}-1)$. The eigenvector is found to be

$$\tilde{u}_n=q_+^{-n+1}-q_+^{n-N},\quad n=0,\cdots,N+1. \tag{3.14}$$

It is antisymmetric with respect to the space, namely, $\tilde{u}_{N+1-n}=-\tilde{u}_n$. When $|\mathrm{Re}\lambda|$ is not small, an eigen-mode is a surface mode, and λ approximately solves (3.12). Moreover, after some algebraic calculations, we find that the only situation for $V_N^+(\lambda)$ and $V_N^-(\lambda)$ to possess a common root is $\lambda=0$ under the condition $\alpha+\beta=0$.

3.2 Unstable surface modes

In this subsection, we seek for a positive eigenvalue λ. Noticing that when $\lambda \geq 0$, we have $q_+ \geq \lambda^2+1$. Hence as $\lambda \to +\infty$, it holds that

$$V_N^{\pm}(\lambda) \sim (\lambda-\alpha) q_+^{N+1} \to +\infty.$$

On the other hand, we observe that $q_+ = 1$ at $\lambda = 0$. It gives $V_N^+(0) = -2(\alpha+\beta)$, and $V_N^-(0) = 0$. We further compute $\frac{dq_+}{d\lambda}(0) = 1$, and

$$\begin{aligned} \frac{dV_N^-(0)}{d\lambda} &= \left\{ q_+^{N+1} - 1 + [(\lambda-\alpha)(N+1)q_+^N - \beta N q_+^{N-1} + \beta] \frac{dq_+}{d\lambda} \right\}_{\lambda=0} \\ &= -[(\alpha+\beta)N + (\alpha-\beta)]. \end{aligned} \tag{3.15}$$

Similarly, we compute for $\lambda = \alpha$.

$$V_N^+(\alpha) = -\beta q_+ (q_+^{N-1}+1), \quad V_N^-(\alpha) = -\beta q_+ (q_+^{N-1}-1). \tag{3.16}$$

By the intermediate value theorem, we find that a positive eigenvalue λ_+ exists for $V_N^+(\lambda_+) = 0$ if $\alpha+\beta > 0$. The eigenvalue $\lambda_+ > \alpha$ if both α and β are positive. There also exists another positive eigenvalue $\lambda_- > 0$ for $V_N^-(\lambda_-) = 0$, if $\alpha + (N-1)\beta/(N+1) > 0$. The eigenvalue $\lambda_- > \alpha$ if both α and β are positive.

For a positive eigenvalue λ, the corresponding $q_+(\lambda) \geq \lambda^2+1$. As discussed in the previous section, it is a root to (3.12). In particular, the difference between λ_- and λ_+ is negligible when N is big. Furthermore, the corresponding eigen-modes are surface modes. We remark that the surface mode is purely a standing wave without propagation, which grows exponentially in time [2, 4, 18, 21].

We further remark that when $\alpha+\beta = 0$, the total energy

$$E(t) = \frac{1}{2}\sum_{n=1}^{N} v_n(t)^2 + \frac{1}{2}\sum_{n=0}^{N} (u_{n+1}(t) - u_n(t))^2$$

decreases if $\alpha < 0$, increases if $\alpha > 0$, and conserves if $\alpha = 0$. The last case corresponds to a fixed boundary.

3.3 Numerical tests

We illustrate the previous analysis by numerical tests. In particular, we take $\alpha = -1, \beta = 2$. The modulus of the reflection coefficient is depicted in Fig. 1. It is less than 1 except at $k = 0$ and π.

For a relatively short lattice with $N = 20$, the 42 eigenvalues are displayed in Fig. 2. There are three types of eigenvalues. First, there are a pair of positive real eigenvalues, giving rise to the unstable surface modes. Even in such a short chain, they are very close. The second type includes two pairs of eigenvalues with real parts about -0.438.

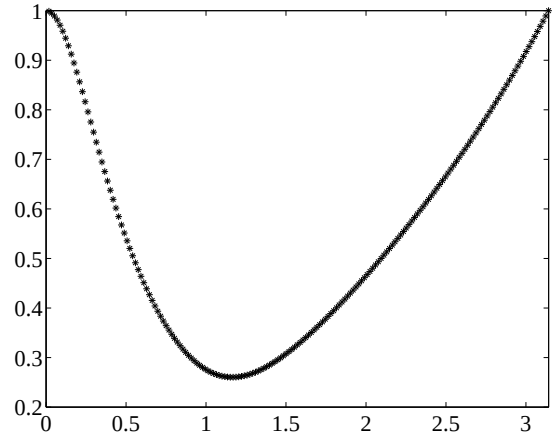

Figure 1: Reflection coefficient for $\alpha=-1,\beta=2$: the horizontal axis denotes the wave number k, and the vertical axis denotes the reflection coefficient $|R|$.

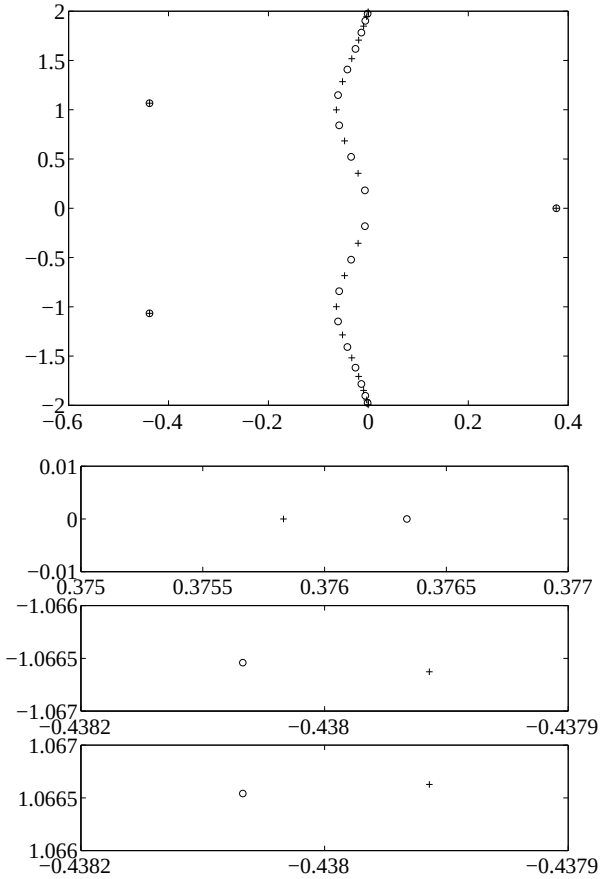

Figure 2: Eigenvalues for $\alpha=-1,\beta=2,N=20$ in the complex plane. The last three subplots are zoom-in view of the 3 pairs of eigenvalues. '+': roots to $V_N^+(\lambda)$; 'o': roots to $V_N^-(\lambda)$.

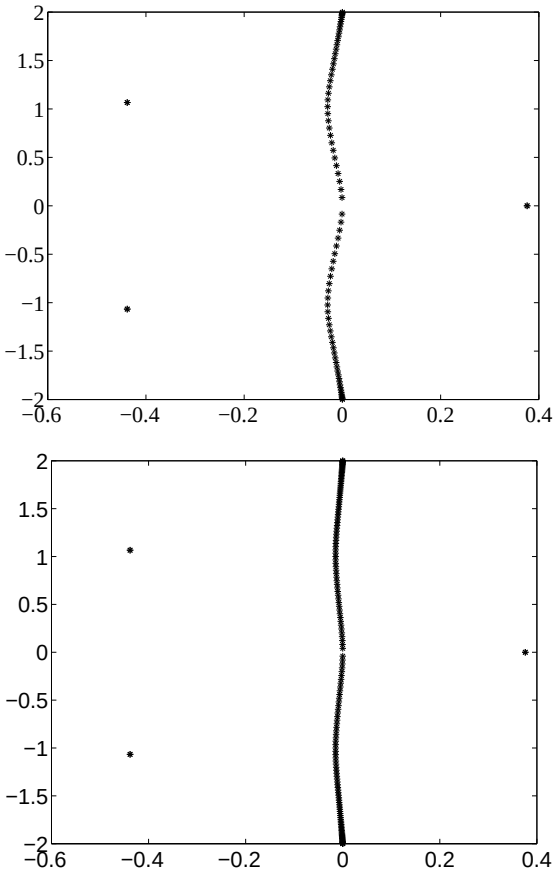

Figure 3: Eigenvalues for $\alpha=-1,\beta=2$ in the complex plane: top $N=40$, bottom $N=80$.

The corresponding eigen-modes are effectively absorbed. We refer to these modes as the absorption modes. The subplots show the details for these eigenvalues. The above three pairs of eigenvalues are approximately the roots to (3.12). The third type, located near the imaginary axis, includes all other eigenvalues. Their real parts are between -0.06398 and -0.00037. The corresponding eigen-modes are stable, and are damped out very slowly. They are referred as vibration/propagation modes. Checking the symmetry for eigenvectors, we may detect whether an eigenvalue is a root to $V_N^+(\lambda)$ or $V_N^-(\lambda)$.

For a longer chain, the first two types of eigenvalues remain unchanged, whereas the third type of eigenvalues get closer to the imaginary axis. See Fig. 3. For instance, the real parts of these eigenvalues are between -0.0301 and -4.716×10^{-5} for $N=40$; and between -0.0146 and -5.914×10^{-6} for $N=80$. More detailed numerical computations show that the minimal real part goes on the order of $\mathcal{O}(N^{-1})$.

Some eigen-modes are displayed in Fig. 4 for a chain with 42 atoms. The two unstable surface modes are shown in the first two subplots. They are real. The exponential decay away from the surface is evident. In contrast, the absorption modes in the next

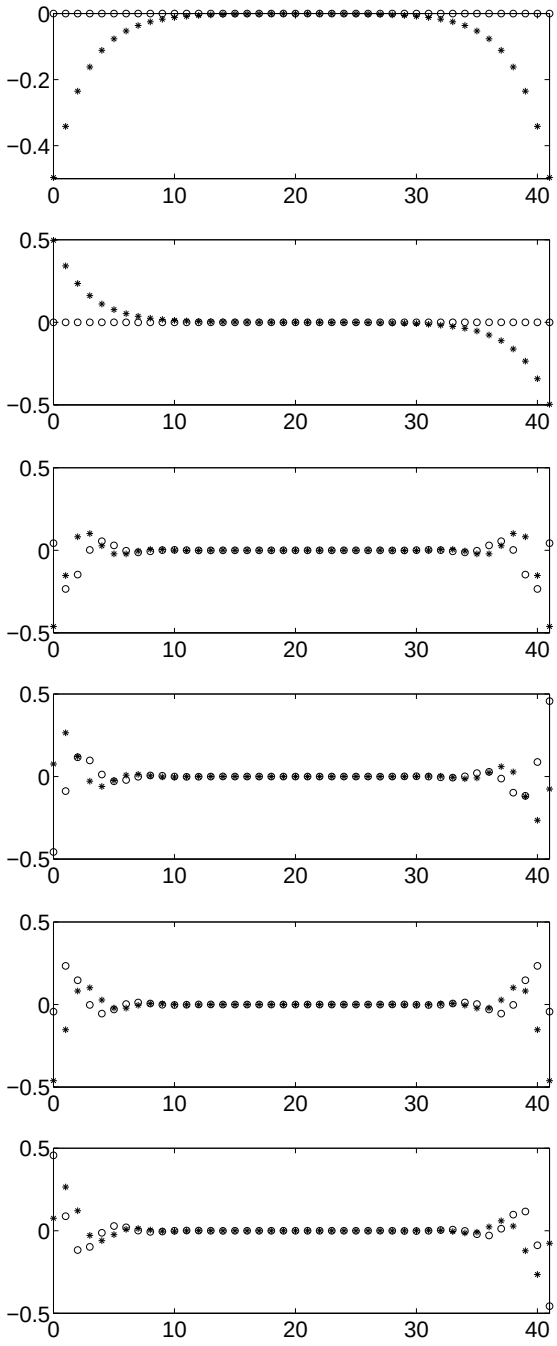

Figure 4: Eigen-modes for a chain with $N=40$: '*' represents the real part, and 'o' represents the imaginary part. Subplots from top to bottom: eigen-mode for eigenvalue 0.376086 of $V_N^+(\lambda)$; eigen-mode for eigenvalue 0.376086 of $V_N^-(\lambda)$; eigen-mode for eigenvalue $-0.43804+1.06658i$ of $V_N^+(\lambda)$; eigen-mode for eigenvalue $-0.43804+1.06658i$ of $V_N^-(\lambda)$; eigen-mode for eigenvalue $-0.43804-1.06658i$ of $V_N^+(\lambda)$; eigen-mode for eigenvalue $-0.43804-1.06658i$ of $V_N^-(\lambda)$.

four subplots are complex, and oscillations present near the boundaries. As in both the unstable modes and the absorption modes the inner atoms are essentially motionless, the instability and absorption are observable only around the boundary. Moreover, the third and fifth subplots are complex conjugates. So for the fourth and sixth subplots. The numerical results verify the previous analysis.

Comparing with the stability condition $\beta>0$ from the reflection coefficient analysis, we observe that instability actually occurs when $\alpha+\beta>0$. The reflection coefficient approach gives irrelevant stability statement for the finite chain. This is due to the fact that the Fourier modes in the form of $\tilde{u}_n=e^{ikn}$ do not comply with the surface modes. Instead of sinusoidal forms, the surface modes have exponential decay profiles. The absorption modes do not have sinusoidal profiles either. Because the basis or general solution to the governing system (2.1a)-(2.1d) differs from the Fourier modes, the reflection coefficient approach naturally does not yield a correct stability result. Though the invalidity of the Fourier modes has been known for a long time, our analysis quantitatively clarify this point and its consequences.

4 Long time instability

We consider a special case when $0<\alpha+\beta\equiv\delta\ll 1$. In addition, we assume that $\delta=o(1/N)$. We expect a very small positive eigenvalue λ corresponding to $V_N^+(\lambda)=0$. Taking a leading order approximation $\lambda=a\delta+o(\delta)$, we easily find that $q_+=1+a\delta+o(\delta)$, and $q_+^N=1+Na\delta+o(\delta)$. Using repeatedly $\delta=\alpha+\beta$, we compute

$$\begin{aligned} V_N^+ &= [(a\delta-\alpha)(1+a\delta)-\beta](1+Na\delta)+[(a\delta-\alpha)-\beta(1+a\delta)]+o(\delta)\\ &= 2(a-1)\delta+o(\delta). \end{aligned}$$

To make $V_+^N(\lambda)=0$, we conclude that $a=1$. That is, $\lambda=\delta$ on the leading order. The positive eigenvalues for some small $\delta=\alpha+\beta$ are listed in Table 1 (all computed with $N=40$). We observe that the dependence on the particular choice of α and β gets weaker as δ decreases. For the last three rows, we have $\delta N=0.04$, and the maximal positive eigenvalues are very close to $\delta=0.001$.

We remark that $\alpha+\beta=0$ is equivalent to the long-wave limit property for a boundary condition in the form of (2.1a) or (2.1d). A minor violation of this condition may lead to a very small yet non-zero eigenvalue. In real applications, particularly when a more complex boundary condition is adopted, the long-wave limit property may likely be slightly violated. If the violation leads to a positive eigenvalue, the long-time instability occurs. This has been observed by some practitioners for absorbing boundary condition computations. Because of the smallness of the eigenvalue, the unstable mode usually reaches an observable magnitude only after a long run, typically long after the main wave package reaches at the boundary and gets well absorbed. Furthermore, if δ is negative instead, the instability does not occur. As the boundary condition with $|\delta|\ll 1$ is viewed as a per-

Table 1: Maximal positive eigenvalue.

$\alpha+\beta$	α	β	$\max\lambda_+$
0.1	-1	1.1	0.0540
0.1	-0.9	1	0.0410
0.1	0	0.1	0.0909
0.01	-1	1.01	0.0085
0.01	-0.99	1	0.0086
0.01	0	0.01	0.0095
0.001	-1	1.001	0.00098
0.001	-0.999	1	0.00098
0.001	0	0.001	0.00095

turbation from $\delta=0$, instability presents only for a positive δ. The complexity makes the long time instability a hidden problem for most calculations.

In the multiscale computation community, the instability is usually regarded as the numerical error accumulation. As a matter of fact, for $\delta<0$, numerical error also accumulates, yet it does not lead to indefinite growth of the total energy. Instead, the total energy is eventually damped out to the level of round-off error. By comparing with the case of $\delta>0$, we show that this weak instability for the boundary condition better explains the phenomenon.

The long time instability occurs not only for the velocity boundary conditions. For instance, with a verlet algorithm to solve the Newton equations at a time step size $\Delta t=1/64$, a dynamic atomistic-continuum method takes the following boundary condition [6]:

$$\begin{aligned} u_0^{k+1} &= \eta u_0^k - 0.074207u_1^k - 0.014903u_2^k - 0.95406u_0^{k-1} \\ &\quad + 0.074904u_1^{k-1} + 0.015621u_2^{k-1}, \qquad (4.1) \\ u_{N+1}^{k+1} &= \eta u_{N+1}^k - 0.074207u_N^k - 0.014903u_{N-1}^k - 0.95406u_{N+1}^{k-1} \\ &\quad + 0.074904u_N^{k-1} + 0.015621u_{N-1}^{k-1}. \qquad (4.2) \end{aligned}$$

Here $u_n^k=u_n(k\Delta t)$, and the coefficient η is suggested as 1.95264 in [6]. With this choice, it may be shown that the energy decays monotonically. However, if we take $\eta=1.95265$ instead, a slow exponential growth appears after a long run. In Fig. 5, we display the calculation for a 401-atom-chain with initial data shown in the second subplot. The waves are effectively absorbed at around $t=200$ when they arrive at both ends. See the fourth subplot at $t=300$. The unstable mode becomes evident at time around $t=700$. In the last subplot for $t=800$, the displacement profile is exactly the unstable eigen-mode. This unstable mode keeps growing later on, and dominates the lattice motion. The growth can be observed clearly from the energy in the first subplot. We remark that the latter choice of η violates the long wave limit property $R(0)=0$. In the original design for the atomistic-continuum method, $R(0)=0$ is taken as a constraint for the reflection mini-

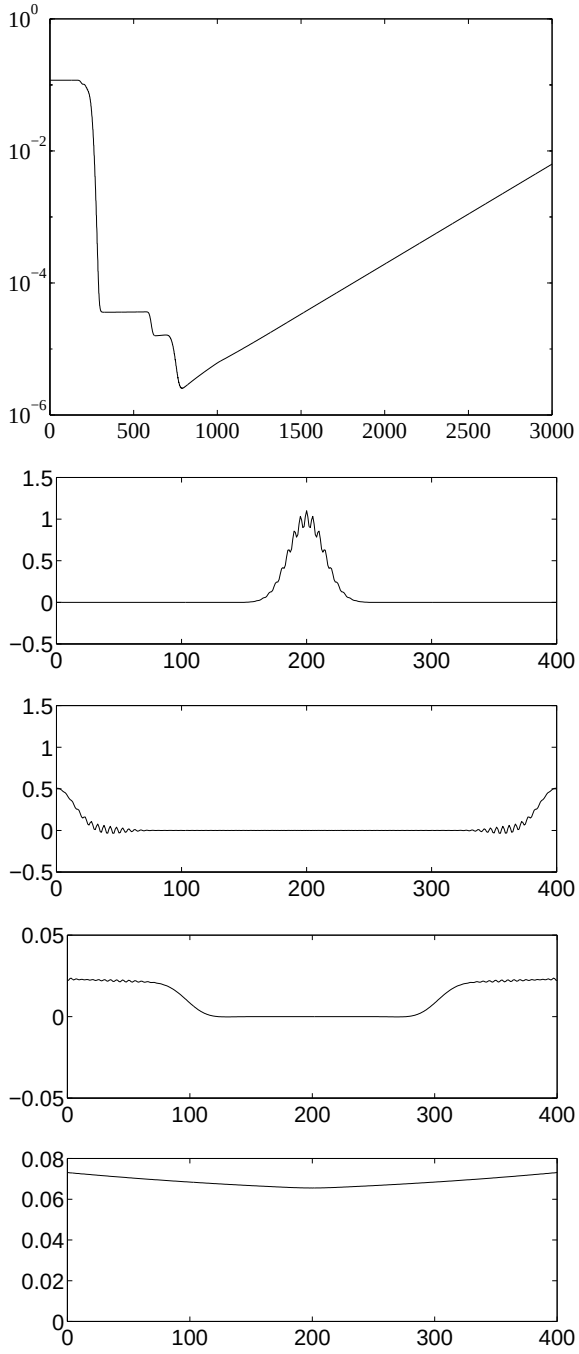

Figure 5: Long time instability in a dynamic atomistic-continuum calculation with a perturbed boundary condition. Subplots from top to bottom: evolution of the total energy (horizonal axis for time); displacements at $t=0$, $t=200$, $t=300$, and $t=800$.

mization problem. With the numerical example, we demonstrate the importance of this constraint.

5 Conclusion

In this study, we check the validity of the reflection coefficient approach, which has been widely adopted in the community of theoretical and computational physics. Through careful explorations on a finite chain under a class of velocity boundary conditions, we have revealed the deficiency of this approach. The cause for the deficiency lies in the known fact that the Fourier modes are not the eigen-modes in general. We discover that unstable surface modes exist with non-sinusoidal profiles, in a parameter range where the reflection coefficient approach claims to be stable. Furthermore, we studied the boundary condition which slightly violates the long-wave-limit property. A very small yet positive eigenvalue may appear, leading to the long time instability, which have been observed by some practitioners.

We would like to remark that this study mainly focuses on the unstable modes. Numerical tests indicate that we do have stability away from the parameter region where the unstable surface modes exist. Furthermore, the existence of such modes may be searched from a low order polynomial, which greatly reduces the complexity of stability analysis. The method we proposed may be extended to more general lattices.

The deficiency of the reflection coefficient approach requires revisits of the wave propagations in physical sciences, as well as numerical algorithms. This may be particularly critical at micro- or nano-scale. Absorbing boundary conditions for wave propagation computations in an unbounded domain, or multi-scale computations with absorbing boundary conditions are two important topics where the fidelity of the reflection coefficient analysis needs better clarified. Moreover, it would be our future work to extend the analysis to the stability in multiple dimensions, on which many important contributions have been made by Li *et al* [16], Liu's group [11, 19, 26] and many other researchers.

Acknowledgments

We are grateful to the anonymous referees for their stimulating discussions. This study is supported in part by NSFC under contract number 10872004, National Basic Research Program of China under contract number 2007CB814800, and the China Ministry of Education under contract numbers NCET-06-0011 and 200800010013.

A Semi-infinite chain

To better understand the deficiency of the reflection coefficient approach, we consider a semi-infinite chain

$$\dot{u}_0 = \alpha u_0 + \beta u_1, \tag{A.1a}$$

$$\dot{u}_n = v_n, \qquad n = 1,\cdots,N,\cdots, \tag{A.1b}$$

$$\dot{v}_n = u_{n-1} - 2u_n + u_{n+1}, \quad n = 1,\cdots,N,\cdots. \tag{A.1c}$$

By a similar argument we find that $u_n(t) = \tilde{u}_n e^{\lambda t}$ with $\tilde{u}_n = Aq_+^n + Bq_-^n$. The boundary condition reads

$$\lambda \tilde{u}_0 = \alpha \tilde{u}_0 + \beta \tilde{u}_1. \tag{A.2}$$

To find the unstable modes, we seek for a real eigenvalue λ. Corresponding to such an eigenvalue, we know from $q_+ > 1$ that $A = 0$ for a motion with a finite total energy. The boundary condition then gives

$$\lambda = \alpha + \beta q_-. \tag{A.3}$$

This algebraic equation is equivalent to (3.10). It has a positive root λ for either $\alpha \leq 1, \beta > -\alpha$; or $\alpha > 1, -\alpha > \beta > -(\alpha + 2\sqrt{\alpha^2+3})/3[2\alpha^2+3-2\alpha\sqrt{\alpha^2+3}]$. The neutral stability curve is depicted in Fig. 6. The eigen-mode has an exact form of $u_n(t) = q_-^n e^{\lambda t}$, which exponentially decays in depth, and exponentially grows in time. Again, the reflection coefficient approach can not account for the instability of the surface modes.

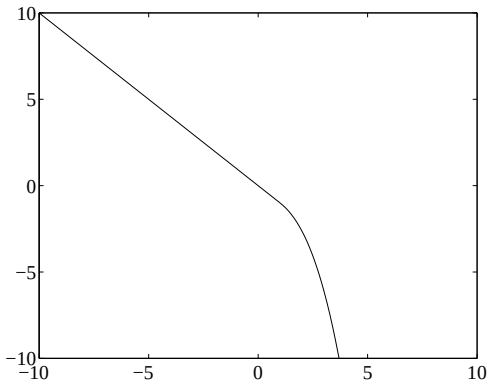

Figure 6: Neutral stability curve for a semi-infinite chain in (α,β) plane. Unstable surface modes exist for parameter above the curve.

B Stability analysis for general boundary conditions

We consider a class of more general boundary conditions.

$$\dot{u}_0 = \alpha u_0 + \sum_{j=1}^{J} \beta_j u_j, \tag{B.1a}$$

$$\dot{u}_{N+1} = \alpha u_{N+1} + \sum_{j=1}^{J} \beta_j u_{N+1-j}. \tag{B.1b}$$

The reflection coefficient is

$$R(k)=-\frac{\Big(\alpha+\sum_{j=1}^{J}\beta_j\cos jk\Big)+i\Big(\sum_{j=1}^{J}\beta_j\sin jk-2\sin(k/2)\Big)}{\Big(\alpha+\sum_{j=1}^{J}\beta_j\cos jk\Big)-i\Big(\sum_{j=1}^{J}\beta_j\sin jk+2\sin(k/2)\Big)}. \tag{B.2}$$

We have $|R|<1$ under the condition

$$\sum_{j=1}^{J}\beta_j\sin jk>0.$$

With the previous $q_{\pm}(\lambda)$, we may find that an eigenvalue is a root to

$$W_N^{\pm}(\lambda)=\left[(\lambda-\alpha)q_+^{N+1}-\sum_{j=1}^{J}\beta_j q_+^{N+1-j}\right]\pm\left[\lambda-\alpha-\sum_{j=1}^{J}\beta_j q_+^{j}\right]=0. \tag{B.3}$$

As $\lambda\to+\infty$, we have $W_N^{\pm}(\lambda)\to+\infty$. At $\lambda=0$, we find that

$$W_N^{+}(0)=-2\Big(\alpha+\sum_{j=1}^{J}\beta_j\Big),\quad W_N^{-}(0)=0,$$

and

$$\frac{dW_N^{-}(0)}{d\lambda}=-\Big[\alpha(N+1)-\sum_{j=1}^{J}\beta_j(N+1-2j)\Big].$$

At $\lambda=\alpha$, we have

$$W_N^{\pm}(\alpha)=-\sum_{j=1}^{J}\beta_j(q_+^{N+1-j}\pm q_+^{j}).$$

Therefore, a positive eigenvalue λ_+ exists for $W_N^{+}(\lambda_+)=0$ if $\alpha+\sum_{j=1}^{J}\beta_j>0$. The eigenvalue $\lambda_+>\alpha$ if both

$$\alpha>0\quad\text{and}\quad\sum_{j=1}^{J}\beta_j(q_+^{N+1-j}+q_+^{j})>0.$$

There also exists another positive eigenvalue $\lambda_->0$ for $W_N^{-}(\lambda_-)=0$, if

$$\alpha-\sum_{j=1}^{J}\frac{\beta_j(N+1-2j)}{N+1}>0.$$

The eigenvalue $\lambda_->\alpha$ if both

$$\alpha>0\quad\text{and}\quad\sum_{j=1}^{J}\beta_j(q_+^{N+1-j}-q_+^{j})>0.$$

The eigenvector corresponding to an eigenvalue that is a root to $W_N^+(\lambda_+)$ is symmetric. Up to a factor, it is

$$\tilde{u}_n = \sum_{j=1}^{J} \beta_j \left(q_+^{N+1-n+j} - q_+^{N+1-n-j} + q_+^{n+j} - q_+^{n-j} \right).$$

The eigenvector corresponding to $W_N^-(\lambda_-)$ is antisymmetric. It may be taken as

$$\tilde{u}_n = \sum_{j=1}^{J} \beta_j \left(q_+^{N+1-n+j} - q_+^{N+1-n-j} - q_+^{n+j} + q_+^{n-j} \right).$$

References

[1] S.A. Adelman, and J.D. Doll, J. Chem. Phys. 61 4242 (1974).
[2] R.E. Allen, G.R. Alldredge, and F.W. de Wette, Phys. Rev. B 4 1648 (1971).
[3] X. Antoine, A. Arnold, C. Besse, M. Ehrhardt, and A. Schädle, Commun. Comput. Phys. 4(4) 729 (2008).
[4] L. Brekhovskikh, and V. Goncharov, Mechanics of Continua and Wave Dynamics, Springer, Berlin, (1985) p. 65-69.
[5] W. Cai, M. de Koning, V.V. Bulayov, and S. Yip, Phys. Rev. Lett. 85 3213 (2000).
[6] W. E, and Z.Y. Huang, J. Comput. Phys.182 234 (2002).
[7] B. Engquist, and A. Majda, Math. Computation 31 629 (1977).
[8] T. Ha-Duong, and P. Joly, Math. Computation 62 539 (1994).
[9] L. Halpern, Math. Computation 38 415 (1982).
[10] E. Herrin, and T. Goforth, Bull. Seismological Soc. Amer. 67 1259 (1977).
[11] E. G. Karpov, G. J. Wagner, and W. K. Liu Int. J. Numer. Methods Engrg. 62 1250 (2005).
[12] R.L. Higdon, SIAM J. Numer. Anal. 31 64 (1994).
[13] J.B. Keller, and D. Givoli, J. Comput. Phys. 82 172 (1989).
[14] H. O. Kreiss, Comm. Pure Appl. Math. 23 277 (1970).
[15] X. Li, J. Comput. Appl. Math. 231 493 (2009).
[16] X. Li, and W. E, Commun. Comput. Phys. 1 136 (2006).
[17] Z.P. Liao, Introduction to Wave Motion Theories in Engineering (2nd ed.), Science Press, Beijing, (2002) p. 136-189 (in Chinese).
[18] A.B. Manenkov, IEE Proc. J. Optoelectronics 139 101 (1992).
[19] H. Park, E. G. Karpov, P. Klein, and W. K. Liu, J. Comput. Phys. 207 588 (2005)
[20] D. Qian, G.J. Wagner, and W.K. Liu, Comput. Methods Appl. Mech. Engrg. 193 1603 (2004).
[21] L. Rayleigh, Proc. London Math. Soc. s1-17 4 (1885).
[22] S.Y. Ren, Phys. Rev. B 64 035322 (2001).
[23] S.Q. Tang, T.Y. Hou, and W.K. Liu, J. Comput. Phys. 213 85 (2006).
[24] S.Q. Tang, J. Comput. Phys. 227 4038 (2008).
[25] A. To, and S. Li, Phys. Rev. B 72 035414 (2005).
[26] G. J. Wagner, E. G. Karpov, and W. K. Liu, Comput. Methods Appl. Mech. Engrg. 193 1579 (2004).
[27] D. Yang, S. Wang, Z. Zhang, and J. Teng, Bull. Seism. Soc. Am. 93 2389 (2003).